JOURNAL OF MATERIALS SCIENCE 35 (2000) 5433–5436

Sintering characteristics and dielectric properties of silver-doped PMN-PZN-PT relaxor ferroelectric ceramics

RUZHONG ZUO, LONGTU LI, RENZHENG CHEN, ZHILUN GUI
The State Key Laboratory of New Ceramics and Fine Processing, Department of Materials Science and Engineering, Tsinghua University, Beijing, 100084, People's Republic of China
E-mail: Ruzhong@mail.cic.tsinghua.edu.cn

The effects of silver doping on PMN-PZN-PT relaxor ferroelectric ceramics were investigated in order to demonstrate the roles of the inner electrodes in the cofiring of MLCCs, because silver could diffuse from an electrode layer into a dielectric layer. Even if the addition of silver promoted the sintering of ceramics, the insulation resistance and the dielectric properties were changed to a certain extent so that they had a great influence on the reliability of MLCCs. Defect chemistry principles were used to analyze the mechanism of action of silver doping. The relationship of silver migration and microstructural formation was also discussed

1. Introduction

With the rapid development of modern electronics and surface mounting technology (abbreviated as SMT), today's electronic devices are progressing in the direction of lighter, thinner, shorter and smaller ones. Multi-layer ceramic capacitors (MLCs) are typical examples because they meet the demand for high capacitance and small size. Due to the inversely-proportional relationship of capacitance with the square of the dielectric layer thickness in MLCCs, many attempts have been made to concentrate on how to produce a thinner ceramic layer. In commercial MLCs today, a dielectric layer is about 10–20μm thick. However, a thinner ceramic layer will be prepared in the near future, which can make the interface more important. This is mainly because of the inter-diffusion and the chemical reaction between dielectric materials and metal electrodes. During the cofiring of Ag/Pd-based MLCCs, the migration of silver has been reported [1–3]. Therefore, it is very interesting to study how the sintering behavior and the dielectric properties of ceramics are affected by silver, which is helpful to understand the influence of the internal electrodes on the cofiring mechanism and the dynamic of multi-layer ceramic devices.

Conventionally, $BaTiO_3$-based dielectrics have been extensively used in MLCCs. Because of their sintering temperature higher than 1300°C, an expensive noble metal such as Pt, Pd and Au must be used as an internal electrode. In contrast to $BaTiO_3$ ceramics, lead-based relaxor dielectrics have been receiving much attention and expected to be the promising dielectrics for MLCCs, due to their anomalously large dielectric constant, large electrostrictive strain, broad dielectric maximum and relatively low firing temperature. PMN-PZN- based relaxors as middle-low-temperature sintering ceramic materials have become increasingly mature. PMN-PZN-PT ceramics, which can be modified by suitable dopants and meet Y5V and Z5U characteristics (EIA specification), have been developed by Li[4] and commercially applied in MLCCs.

The purpose of this paper is to investigate the effects of silver doping on the physical and dielectric properties of PMN-PZN-PT relaxors based MLCCs. The roles of silver diffusion are estimated by using silver-doped disk specimens.

2. Experimental details

The main constituents of the studied samples were xPMN-yPZN-zPT ($x+y+z=1$, $0.9<x<0.95$, $0<y<0.05$, $0<z<0.1$), modified by a small amount of MnO_2, MgO and other dopants. This system has a characteristic of Y5V or Z5U in MLCCs and can be sintered in a wide range of 880–1000°C. The preparing process has been described elsewhere [5]. The calcined ceramic powders and $AgNO_3$ solid were weighed and mixed by ball-milling in de-ionized water for 24 h, assuming the homogeneous distribution of silver in the mixture. The dried powders were pressed into 10-mm-diameter disk pellets under 2 MPa pressure and sintered at 980°C for 3 h in a closed alumina crucible using a protective Pb atmosphere.

The fracture morphology and the grain size were determined by a scanning electron microscope (SEM, JEOL6301F). The density of the fired samples was measured according to the Archimedes principle. The sintering densification curves were obtained according to the change in size.

The dielectric constant and the loss value of the specimens were measured pseudo-continuously at 1 V_{rms} and 1 kHz at the temperature of −60°C–130°C using an

impedance analyzer (HP4192), a Delta2300 automatic temperature control box and a computer-monitoring system. The powder X-ray diffraction was used to confirm the phase formation in the samples as sintered. The insulation resistance was measured by applying 100 v voltage to the specimens for 1 min at room temperature.

3. Results and discussion

3.1. Sintering characteristics and physical properties of silver-doped samples

The sintering characteristic was examined as a function of silver doping in the fired samples. Fig. 1 showed that the sintered density increased slightly with doping a small amount of silver. The density of all the samples was higher than 7.70 g/cm^3, and more than 98 percent of theoretical density. The density of undoped specimens reached about 7.72 g/cm^3, however, it increased to 7.78 g/cm^3 with doping 0.2 mol% silver and reached 7.8 g/cm^3 with doping 0.8 mol% silver.

SEM observations in Fig. 2 showed that the grain size was also dependent on the silver concentration, which had been confirmed elsewhere [6]. This is just like that there is a larger grain size near the internal interfaces than that far away from the electrodes in MLCs. Moreover, the densification of silver-doped samples was greatly improved, as indicated in Fig. 3. The roles of silver in the microstructural formation may have many different explanations. It can be considered that the melting of silver led to the transient liquid sintering. Another outlook is that the reaction of silver with ceramic oxides generated low-melting-point materials, such as Ag-Pb compounds. The two aspects may be considered to simultaneously promote the sintering of the samples. In addition, the grain boundary phase present caused the change in fracture modes from a transgranular fracture to an intergranular fracture because of a week bond between the grains, as shown in Fig. 2. The formation mechanism of the grain boundary phase will be explained in the end.

Fig. 4 indicated that the insulation resistance was changed with the extent of silver doping. This change may be in correlation with the state of silver in the samples. During sintering, silver ion can be incorporated into a growing perovskite grain, occupying the A site because of the same radii of monovalent silver ions as those of divalent lead ions (0.149 nm), but much larger than for B-site cations, such as Nb^{5+}(0.064 nm)

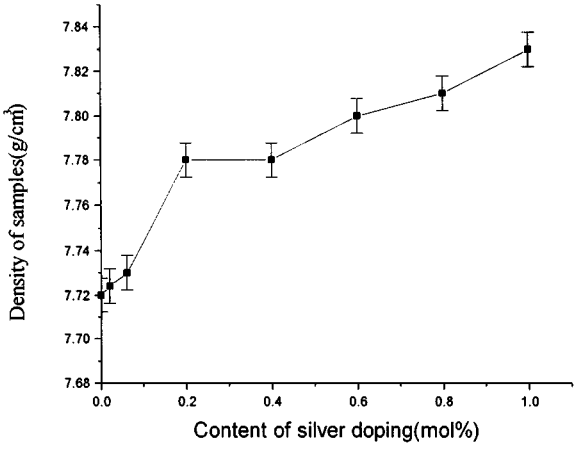

Figure 1 Effect of silver concentration on the density of the samples as fired at 980°C for 3 h.

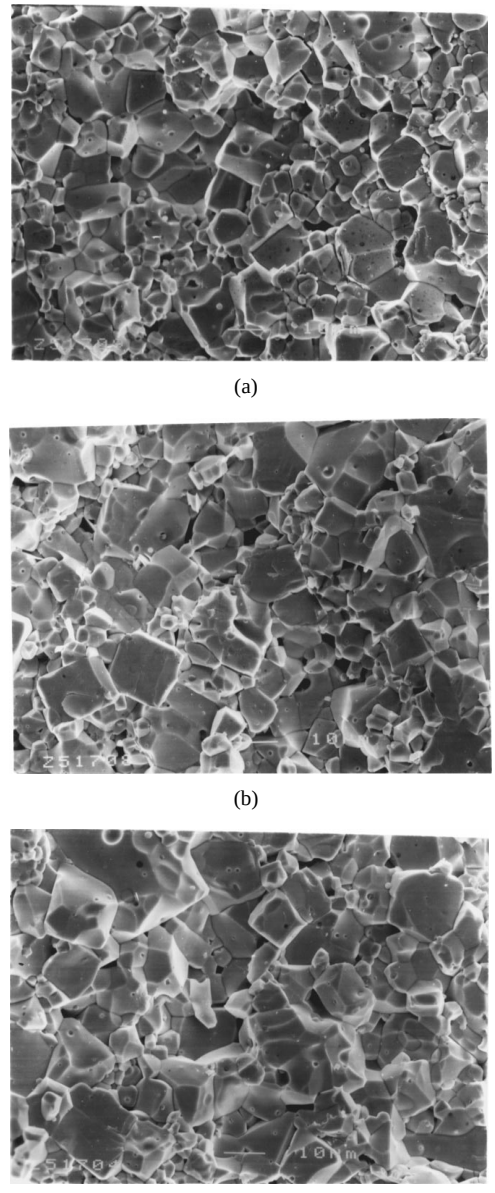

Figure 2 The fracture morphology of silver-doped samples sintered at 980°C for 3 h (a, b, c stands for 0, 0.06, 0.2 mol% silver, respectively).

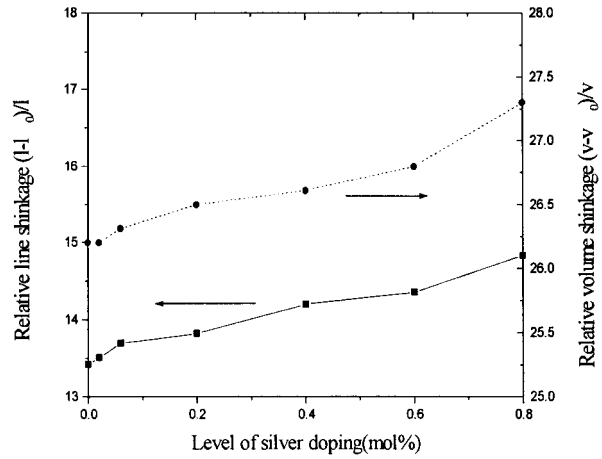

Figure 3 Sintering shrinkage as a function of silver doping.

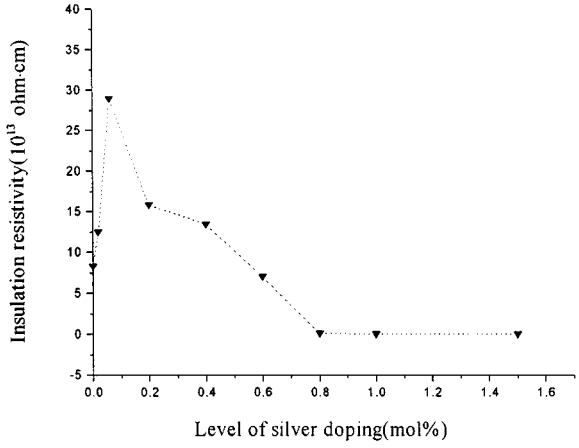

Figure 4 Insulation resistance of silver-doped samples as a function of silver concentration.

and Zn^{2+}(0.074 nm) [7, 8]. According to the above assumption, the unequal-valent substitution of Ag^{+} for Pb^{2+} leads to the appearance of free electrons while oxygen vacancy $V_o^{\cdot\cdot}$ will be produced in order to keep neutral. When an electric field was applied, these electrons could form leakage currents due to their transition from one place to another. It is very interesting that there exists a mico-peak in the curve of Fig. 4. It may be difficult to give a desired interpretation about this. Even though the increase of *R*, due to silver doping, was also previously reported, any reasons were not given. Here, we think that the grain growth and the density rise are responsible for the increase.

3.2. Effect of silver doping on dielectric properties

The dielectric properties of the samples were evaluated as a function of silver concentration. Seen from the Fig. 5, the effect of silver on the dielectric constant was more complex, not monotonically rising or falling, than previously reported [9]. As mentioned above, at first the grain growth made the dielectric constant increase because it led to a reduction in the number of grain boundary with a low *K* in series. On the other hand, with more silver doping, the proportion of the second phase rich in Pb at grain boundary increased, causing the degradation of the dielectric constant. Chen *et al*. [10] also noted that the decrease in *k* vaule could be attributed to a secondary phase consisting of different kinds of oxides with a low K. Besides, Yuichi Sato *et al*. [11] explained the reduction in K_{max} value according to the order-disorder transition of B-site cations.

Generally specking, the substitution of some elements in A-site or B-site of Pb-based perovskites may change the Curie temperature (T_c) [12–15]. As shown in Fig. 6, T_c was reduced with silver doping. T_c of the reference specimen was about 17°C, but it fell to 15.8°C for the samples doped with 0.02 mol% silver, and then decreased to about 13°C when doped with 0.08 mol% silver. We think that the change in T_c is due to the substitution of doped elements into the lattice. The above result also indicated that silver had entered into the lattice of PMN-PZN-PT perovskites to a certain extent. A further proof about silver entering into the lattice can be obtained form XRD spectra in Fig. 7. The main diffraction peaks of silver-doped samples were moved to higher angle. The diffraction angles corresponding to the facial index were listed in Table I. The movement of main diffraction peaks is the result of the lattice contract in terms of the formation of $V_o^{\cdot\cdot}$. Even if silver could be identified to enter into the lattice, any new phases were not found. The spectra also verified the

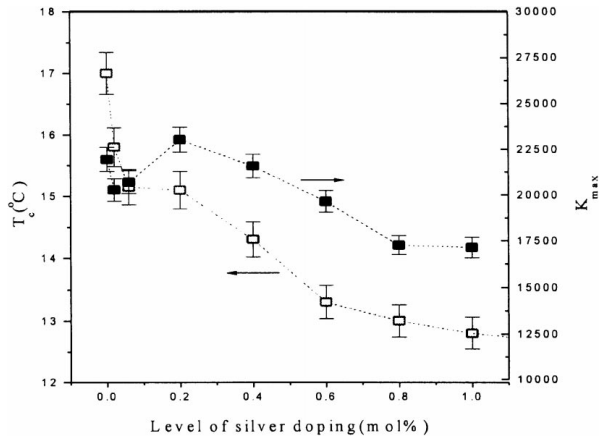

Figure 6 Effect of silver doping on T_c and K_{max} for the samples sintered at 980°C for 3 h.

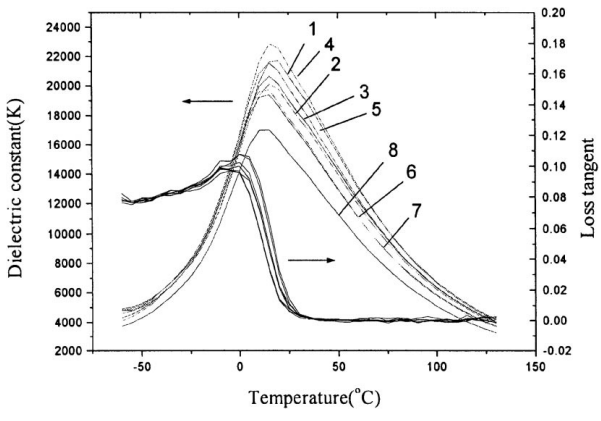

Figure 5 Temperature dependence of the dielectric properties for silver-doped samples sintered at 980°C for 3 h (1–8 stands for 0, 0.02, 0.06, 0.2, 0.4, 0.6, 0.8, 1.0 mol%, respectively).

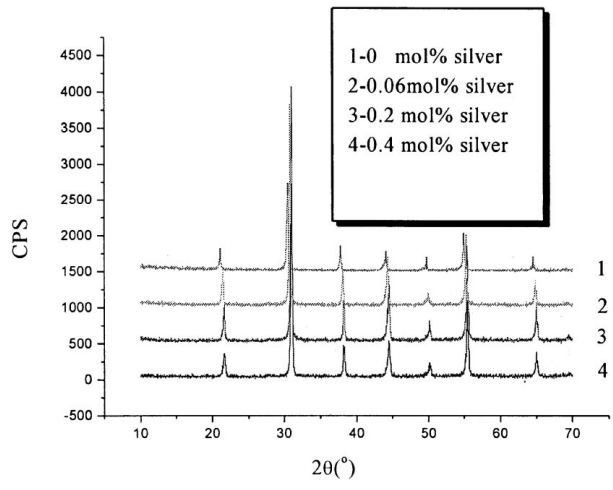

Figure 7 XRD spectra of silver-doped specimens fired at 980°C for 3 h.

TABLE I (authors: Ruzhong Zuo, Longtu Li, Renzheng Chen and Zhilun Gui)

	Facial			Index			
2θ	100	110	111	200	210	211	221
0	21.08	30.48	37.80	44.06	49.68	54.90	64.58
0.04 mol%	21.48	30.80	38.12	44.36	49.96	55.22	64.82
0.2 mol%	21.85	30.98	38.20	44.48	50.10	55.40	65.00
0.4 mol%	21.86	31.00	38.20	44.48	50.12	55.42	65.02

nearly complete perovskite phase, which was not also the same as previously reported [12]. In addition, the substitution of silver for lead inevitably expelled lead atom from the lattice of the perovskites, causing rich-Pb secondary phase to be formed at the grain boundary, as mentioned above.

4. Conclusions

The sintering characteristic and dielectric properties of silver-doped specimens as sintered were investigated. Silver was found to enter into the lattice of the perovskite, causing the shrinking of the lattice and the formation of Pb-rich grain boundary phases.

Due to the low melting point of silver and the secondary phase formed at grain boundary, the sintering properties of silver-doped PMN-PZN-PT relaxor ferroelectric ceramics were improved greatly. The grain size and density of silver-doped samples were enhanced to a certain extent. However, the insulation resistance was changed, which degraded the reliability of MLCCs.

The effects of silver doping on the dielectric properties can be summarized as follows. With a less amount of silver doping, the maximum dielectric constant (K_{max}) was increased, but more silver doping could cause K_{max} to drop. Due to the substitution of silver, T_c decreased monotonically with silver doping.

Acknowledgements

This work was supported by National Natural Science Foundation of China. (Serial Number: 59995523).

References

1. C. H. LU and J. Y. LIN, *Ceramic International* **23** (1997) 223.
2. W. WERSING, H. WAHL and M. CHNÖLLER, *Ferroelectrics* **87** (1998) 271.
3. S. S. COLE, W. H. PAYNE, J. MILLER and V. VENKATESSIN, in the 81st Annual Meeting of the American Ceramic Society, Cincinnati, OH, May 1979.
4. L. T. LI and Z. L. GUI, P. R. China Patent 1, 118, 773, Tsinghua Univ. (1995).
5. Z. L. GUI, P. S. CUI, Y. WANG and L. T. LI, "Advanced Structural Materials" (Elsevier Science Publisher, 1991) p. 463.
6. C. CABALLERO, E. NIETO, P. DURAN and G. DRAZIC, *J. Mater. Sci.* **32** (1997) 3257.
7. R. D. SHANNON, *Acta Crystallogr., Sect. A. Found. Crystallogr* **32** (1976) 751.
8. H. KANAI, M. YOSHI and Y. YAMASHITA, *J. Am. Ceram. Soc.* **77** (1994) 2229.
9. H. KANAI, O. FURUKAWA, S. NAKAMURA, M. HAYASHI, *ibid.* **78** (1995) 1173.
10. J. CHEN, H. H. CHAN and M. P. LIANER, *ibid.* **72** (1989) 593.
11. Y. SATO, H. KANAI, and Y. YAMASHITA, *ibid.* **79** (1996) 261.
12. M. S. CHU and C. E. HODGINS, in "Advances in Ceramic, Vol. 19: Multilayer Ceramic Devices," edited by J. B. Blum and W. R. Cannon (American Ceramic Society Columbus, OH, 1986) p. 203.
13. H. IKUSHIMA and S. HAYAKAWA, *Jpn. J. Appl. Phys.* **4** (1965) 328.
14. K. V. R. MURTY, S. N. MURTY, K. C. MOULI and A. BHANUMATHI, in Proceedings of the IEEE 1992 International Symposium on Applications of Ferroelectrics (Institute of Electrical and Electronics Engineers, Piscataway, NJ. 1992) p. 144.
15. C. H. MAHER, *J. Am. Ceram. Soc.* **66** (1983) 408.

Received 3 June 1999
and accepted 30 March 2000